Risk Assessment of Migration from Packaging Materials into Foodstuffs

O. Vitrac
UMR Fractionnement des Agro-Ressources et Emballage, INRA 614, 51687 Reims Cedex 2, France

M. Hayert
UMR Génie des Procédés Environnement et Agro-alimentaire, CNRS 6144, ENITIAA, 44322 Nantes Cedex 3, France

DOI 10.1002/aic.10462
Published online February 28, 2005 in Wiley InterScience (www.interscience.wiley.com).

This work proposes a generic quantitative methodology to assess the risk of the migration of chemicals from packaging materials into foodstuffs. The distribution of the concentration in food is derived from a stochastic resolution of dimensionless transport equations accounting for physical properties of the considered food product(s) (solid/liquid, volume), of the packaging material(s) (polymer type, thickness), and of possible migrants (initial concentration, diffusion and partition coefficients at the temperature of storage). Each parameter is decomposed as a product of a scale factor and a dimensionless random contribution with known distributions (normal, log-normal, Weibull, gamma, and beta). Nonlinear dependencies between all parameters (up to 12) are reliably handled based on projection techniques and convolution products. The proposed methodology is illustrated on three arbitrary classes of packed food products combined with two migration scenarios and three typical boundary conditions (solid food, liquid food, no-external transport resistance). Finally, data analysis abacuses are provided to appraise the migration risk for more general cases. © 2005 American Institute of Chemical Engineers
AIChE J, 51: 1080–1095, 2005
Keywords: risk assessment, diffusion, packaging, stochastic modeling

Introduction

For the last 20 years, consumers' exposure to chemicals from food packaging materials has attracted much public attention and interest of European regulation authorities because somewhat high concentration levels of substances released by packaging materials were found in several food articles including, in particular, plasticizers released from poly(vinyl chloride) (PVC) cling-films[1-3] or printing inks[4] and bisphenols or derived compounds with epoxy or chlorhydrin group released from can coatings/varnishes, polycarbonate bottles, and sealants.[5-7] Such molecules are known to be potentially carcinogenetic to humans[8] and endocrine disruptors.[9] Harmonization of European regulations relating the principle of inertia of food contact materials (FCM) is quite recent and still under investigation since the general framework directive was published 14 years ago.[10] Current European Union (EU) regulation is based on the concept of a positive list that describes which monomers and additives are authorized and their conditions of use regarding a specific or global migration criterion into food articles. Moreover, EU regulation requires the manufacturer of a new substance or packaging to notify the appropriate authority and to carry out a risk assessment based on migration quantification, toxicity data (such as cytotoxicity, mutagenesis, estrogenic activity), and comparison with existing or proposed daily intake levels. Today such an approach has many drawbacks. First, it entails high effort expenditure and schedule time regarding competitiveness and innovation criteria and esti-

Correspondence concerning this article should be addressed to O. Vitrac at olivier.vitrac@reims.inra.fr.

mates risk only on the basis of worst-case assumptions on both migration and consumption. Second, it may not be used for unknown substances such as those that result from degradation or reactions of primary substances.[5] An alternative would be based on a realistic estimation of the daily intake from a duplicate diet or a stochastic approach. Now, the latter seems more promising because it makes it possible to assess exposure for both average and high consumers, and to take into account the exposure to a combination of substances from different packaging and present in different food products. However, the number of published studies on contamination data is limited, given the analytical difficulties with the analysis of contaminants at very low concentration and in real foodstuffs (that is, multiconstituent and multiphasic materials).

Recent conclusions of a European thematic workgroup,[11] in which one of us participated, demonstrated that for certain FCM our knowledge of both molecular diffusion and macroscopic molecular diffusion coefficients (noted D) was sufficient to foresee the possible contamination of food by substances from packaging for regulation purposes. Thus the aim of this work was to devise a novel and cost-efficient tool, called MIGRARISK, based on knowledge-driven models for the estimation of the risk of chemical contamination of food products by substances originating from FCM. The originality of the approach results in a probabilistic resolution of transport equations that makes it possible to assess the contamination for (1) a particular migrant or (2) migrants with similar chemical structure (such as monomer, antioxidant, plasticizer, and so on) from several FCM and/or into different food products (that is, specific or global exposure from FCM).

To make the statement rigorous, we first introduce a dimensionless and general physical model that may be used to describe realistically most of the migration situations that may be occur between FCM and either solid or liquid foodstuffs. In particular, a general boundary condition is applied to account for both "thermodynamic" and mass transfer resistances at the FCM–food interface. In a second section, from physical considerations and compilation of results from probability theory, we derive statistical laws of the contamination of packed food products, assuming that there are no reaction and mass losses within the FCM and food. In particular, it is demonstrated that the risk of contamination is distributed according to well-known exponential family distributions. However, given that the final probability still depends in the general case on 11 parameters, a dedicated and iterative scheme of risk assessment, based on numerically calculated diagrams, is presented.

Because our mechanistic contamination model is developed independently from the consideration of the availability of data, a simplified approach—based on classes of packed food products and contamination cases—is proposed in a third section. Classes based only on dimensionless statistical criteria provide a convenient and rigorous framework for risk assessors and managers to deal with both variability and uncertainty generated by missing, incomplete, noncomparable, or biased information sources. Because the process of class definition is an iterative process, wherein initial choices may be refined, modified as the insight in the underlying process grows and the availability of data is explored in greater depth, generic dimensionless abacuses are provided in a final section to allow the definition of any new class or application (geometry, composition, variability, handling in private households, and so on).

Physical Formulation of the Transport of Substances between FCM and Foodstuffs

At the molecular scale and at very low concentration, the subsequent transports of a migrant (such as monomer, additive, and residue) within the solid phase (that is, FCM, assumed to be a polymer) and into a liquid or semiliquid phase (that is, food) are related to a process of tracer diffusion in a homogeneous equivalent medium. A migrant is spread through the matrix as the result of the random thermal agitation of both intermingling migrant molecules and polymer segments.[12]

Macroscopic transport equations

As a result, the concentration in a migrant at time t within FCM, with characteristic length scale l along the main transport direction x, is macroscopically controlled by a Brownian density u, defined by the following scaled transport equation

$$\frac{\partial u|_{x^*}^{Fo}}{\partial Fo} = \frac{\partial^2 u|_{x^*}^{Fo}}{\partial (x^*)^2} \tag{1}$$

where $Fo = D \cdot t/l^2$ and $x^* = x/l$ are dimensionless time and position, respectively. D has units in $[l]^2 \cdot [t]^{-1}$ and is assumed uniform and constant within FCM.

At $x^* = 0$, an impervious boundary or symmetry plane condition is assumed. At $x^* = 1$, the scaled flux of u between FCM and food, noted as j^*, is obtained by introducing a generalized boundary condition (Robin BC) that accounts for possible partition effects and for a mass transfer resistance controlled by hydrodynamic conditions between the packaging material and the food product assumed to be either liquid or semiliquid. In the solid case, it is related only to a contact resistance. If no reactions and losses are assumed and if u is defined regarding a mass referential, the corresponding BC is written as

$$j^* = -\left.\frac{\partial u}{\partial x^*}\right|_{x^*=1} = Bi \cdot K(u|_{x^*=1} - u|_{x^*\to\infty}^{Fo=0}) - Bi \cdot L \int_0^{Fo} j^*(\tau) d\tau \tag{2}$$

where $Bi = h_F \cdot l/D$ is a dimensionless number that compares the values of transport resistances between FCM and food, h_F is the equivalent conductance of the latter with units in $[l] \cdot [t]^{-1}$; K is the partition coefficient between FCM and food that describes a possible discontinuous distribution of the migrant $x^* = 1$ for $K \neq 1$; $L = (\rho l)/(\rho_F l_F)$ is the dilution coefficient with ρ/ρ_F the ratio of density between FCM and food; and l_F is the food product equivalent dimension and defined by its reciprocal specific surface area with FCM.

State space considerations

Because Eqs. 1 and 2 are based on a macroscopic description of transport between FCM and food, j^* verifies macroscopic conditions of irreversibility: (1) $j^* > 0$ if $u\,|_{x^*=1} > u\,|_{x\to\infty}^{Fo=0}$ and (2) j^* is monotonically decreasing from an initial value BiK toward 0 when $Fo \to \infty$. As a result, for any migrant with initial density in the FCM $u(x^*, Fo = 0)$ such that $\int_0^1 u(x^*, Fo = 0) dx^* = 1$ and $u\,|_{x\to\infty}^{Fo=0} = 0$, its probability to be still present in

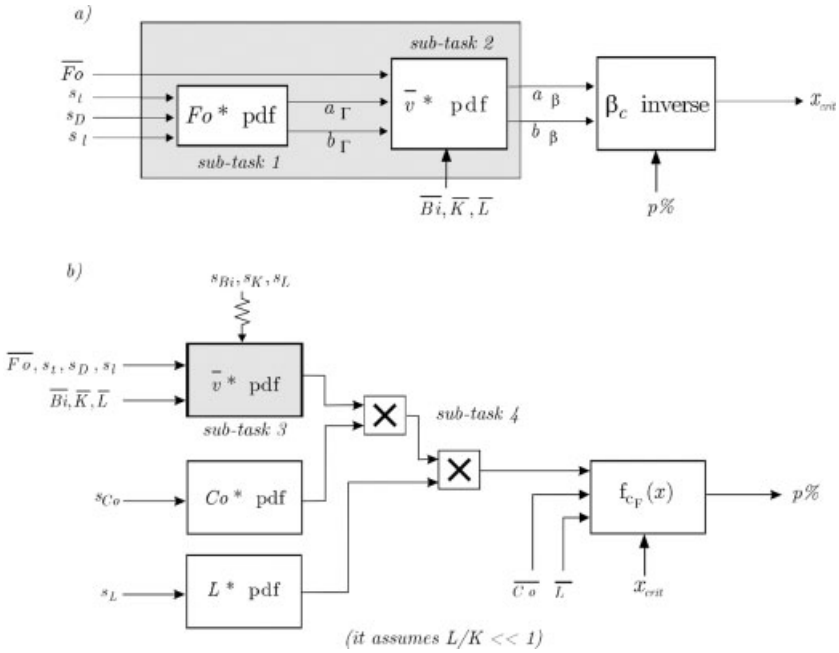

Figure 1. Algorithms for the calculation of (a) the pdf and percentile values of $\bar{v}$*; (b) the pdf of c_F.

the FCM after the scaled duration Fo, defined as $\bar{u} = \int_0^1 u(x^*, Fo)dx^*$, decreases such that

$$\left\{\begin{array}{l} \bar{u} + \displaystyle\int_0^{Fo} j^*(\tau)d\tau = \bar{u} + \frac{\bar{v}}{L} = 1 \\ \bar{U}(Fo \rightarrow \infty) + \displaystyle\int_0^{\infty} j^*(\tau)d\tau = \bar{u}_\infty + \frac{\bar{v}_\infty}{L} = \frac{\bar{v}_\infty}{K} + \frac{\bar{v}_\infty}{L} = 1 \end{array}\right\} \tag{3}$$

where $\bar{v}$ is the equivalent space-averaged Brownian density in the foodstuff (assumed to be homogeneous far from a possible boundary layer at the FCM–food interface).

The combination of expressions in Eq. 3 provides scaled concentration quantities, or state variables, $\bar{u}^* = \bar{u}/\bar{u}_\infty$ and $\bar{v}^* = \bar{v}/\bar{v}_\infty$ (also called migration rate) that are independent of both initial and final states and that are from either technological or thermodynamic considerations. The so-defined state variables are related by the following equation

$$\frac{\bar{v}_\infty}{K}\bar{u}^* + \frac{\bar{v}_\infty}{L}\bar{v}^* = 1 \tag{4}$$

Statistics of the Contamination of Foodstuffs

*Statistics of the migration rate: $\bar{v}$**

The transport from FCM into foodstuffs is thus correspondingly described as a collection of independent jumps at the FCM–food interface. For the same initial and final states [assumed to be $\bar{u}(Fo = 0) = 1$ and $\bar{v}(Fo \rightarrow \infty) = \bar{v}_\infty$], the probability of a jump to occur at time Fo within the scaled time interval dFo is $j^*(Fo)dFo = -(\bar{v}_\infty/K)d\bar{u}^* = (\bar{v}_\infty/L)d\bar{v}^*$. The ratios $\bar{v}_\infty/K$ and $\bar{v}_\infty/L$ are scaling factors, which relate the convenient state variables, $\bar{u}^*$ and $\bar{v}^*$, to the probabilities of occupation in FCM and food, respectively.

Because the ratio $(1 - \bar{v}^*)/(\bar{u}^* - 1) = L/K$ is constant whenever $Fo \geq 0$, the probability $\{pr(\bar{v}^* \leq x)\}_{0\leq x\leq 1}$ with bound support [0, 1], denoted as $F_{\bar{v}^*}(x)$, verifies symmetry properties

$$\left\{\begin{array}{l} Fv^*(x) = pr(\bar{v}^* \leq x) = 1 - pr(1 - \bar{v}^* \leq 1 - x) \\ \quad = 1 - F_{1-v^*}(1 - x) \\ Fv^*(x) = pr(\bar{v}^* \leq x) = pr(1 - \bar{v}^* > 1 - x) \\ \quad = F_{1-v^*}(x) \end{array}\right\}_{0\leq x\leq 1} \tag{5}$$

Such conditions are sufficient to postulate reasonably that the probability $\{pr(\bar{v}^* \leq x)\}_{0\leq x\leq 1}$ follows a cumulative Beta distribution $\beta_c(a_\beta^{\bar{v}^*}, b_\beta^{\bar{v}^*})$, irrespective of the distribution of Fo. The probability of a jump occurring before the scaled time Fo follows a generalized truncated Beta distribution, although this last result will not be used herein because the state variable $\bar{v}^*(Fo, Bi, K, L)$ will be used as a predictor of food contamination data.

Statistics of the contamination of packed food articles: c_F

The contamination of foodstuffs c_F, expressed with the usual concentration units (in mass of migrant per mass of food), is given by

$$c_F(Fo, Bi, K, L) = c_0 \cdot \bar{v}_\infty(K, L)\bar{v}^*(Fo, Bi, K, L) = \frac{c_0}{\frac{1}{K} + \frac{1}{L}}\bar{v}^*(Fo, Bi, K, L) \tag{6}$$

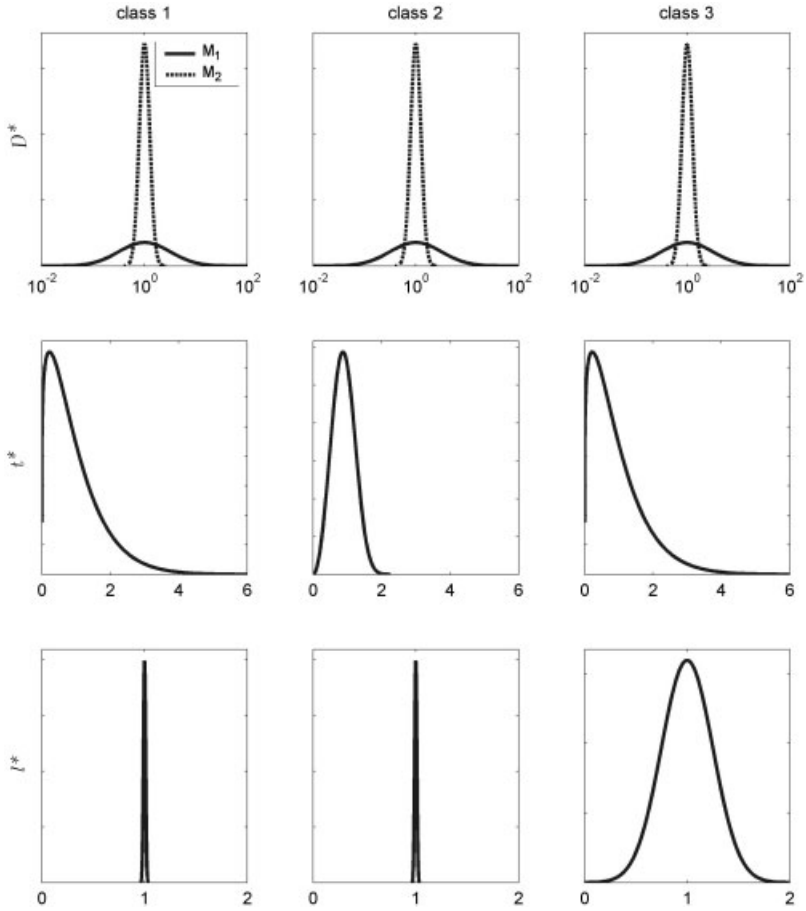

Figure 2. Definition of the three classes of packed food based on the combination of typical pdfs of dimensionless random variables: *D, *t**, *l**.**

Two hypotheses are considered: M_1, nonspecific migrant or equivalently poorly known D value ($s_D = 0.5$); M_2, specific migrant with a well-known D value ($s_D = 0.1$).

where c_0 is the initial migrant concentration in FCM (with the same units as c_F).

If c_0, K, and L have low dispersion, it is expected that the probability density function (pdf) of c_F, defined as $f_{c_F}(x)$, exhibits a priori a highly dissymmetric shape as does the Beta distribution. It is worth noting that this conclusion is independent of kinetic dimensionless numbers Fo and Bi because the hypothesis of a Beta distribution for $\bar{v}^*$ is derived only from global balance considerations that postulate no conflicting situation between a migrant within the FCM and within the food product.

By contrast, the transition from one J-shaped pdf to a reverse one by a moving unimodal pdf depends on Fo, given that $\bar{v}^*$ monotonously increases with Fo. The U shape corresponding to a pdf with both a mode and an antimode is less probable, but still physically consistent, because all critical values (also known as percentile values) of c_F are intuitively expected to increase irreversibly when any moment of Fo increases. For small Fo values, $pr(c_F = x)$ thus decreases exponentially toward zero with a maximum that may be different from 0 if $pr(c_F = 0)$ is negligible. The critical situation $pr(c_F = 0) \approx 0$ corresponds to a particular case where the principle of inertia between FCM and food has no more statistical meaning. For large Fo values, symmetric situations may occur and the $\bar{v}^*$ pdf is maximum for $x \approx [(1/K) + (1/L)]^{-1}$.

If c_0 and/or dimensionless parameters K and L are not δ distributed (that is, with small dispersion), c_F will deviate from the Beta distribution and is more likely to have exponentially damped power tails. If $f_{c_0}(x)$ is the continuous pdf of c_0, $f_{c_F}(x)$ is given by

$$f_{c_F}(x) = \int_0^1 \frac{1}{y} f_{c_0}\left[\left(\frac{1}{K} + \frac{1}{L}\right)\frac{x}{y}\right] \beta_{(a_\beta^{\bar{v}*}, b_\beta^{\bar{v}*})}(y)\,dy \qquad (7)$$

where $\beta_{(a_\beta^{\bar{v}*}, b_\beta^{\bar{v}*})}(x)$ is the Gamma pdf with parameters $a_\beta^{\bar{v}*}$, $b_\beta^{\bar{v}*}$ ($a_\beta^{\bar{v}*} > 0$, $b_\beta^{\bar{v}*} > 0$) and $f_{c_0}(z)\beta_{(a_\beta^{\bar{v}*}, b_\beta^{\bar{v}*})}(y)$ is the joint pdf of

Table 1. Tested Boundary Conditions*

Boundary Condition	$\overline{Bi}$	$\bar{K}$	$\bar{L}$	$\bar{v}_\infty = \left(\frac{1}{\bar{K}} + \frac{1}{\bar{L}}\right)^{-1}$
BC_1	1	0.1	1/50	1/60
BC_2	10	0.5	1/50	1/52
BC_3	10^3	1	1/50	1/51

*BC_1: solid food with low migrant affinity; BC_2: semiliquid food with medium migrant affinity; BC_3: stirred liquid food with good migrant affinity.

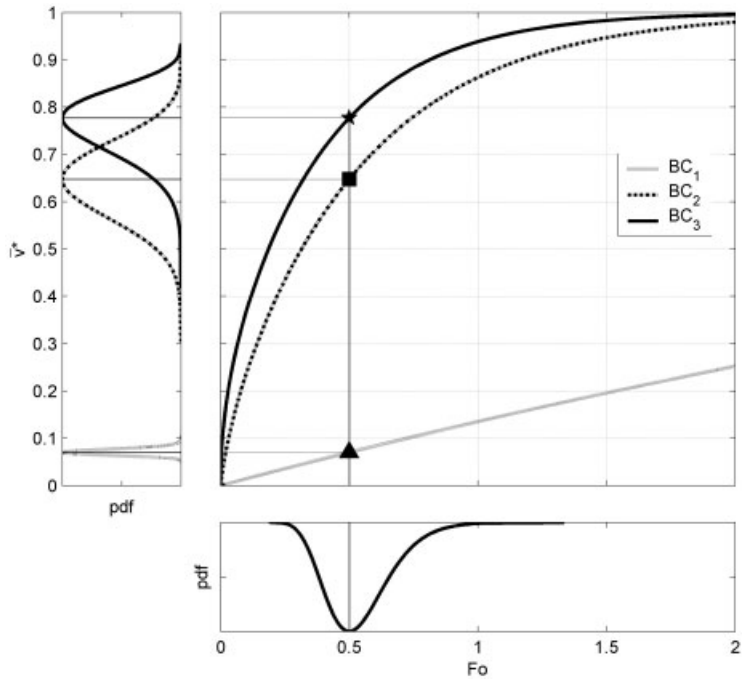

Figure 3. Scaled migration kinetics with respect to tested boundary conditions: BC_1, BC_2, and BC_3 (see Table 1).
The corresponding pdf of $\bar{v}^*$ in response to a given *Fo* pdf defined by $\overline{Fo} = 0.5$, $s_D = 0.1$, $s_t = \infty$, $s_l = 0$ are also plotted.

independent variables c_0 and $\bar{v}^*$. In particular, if c_0 is absolutely continuous and strictly nonnegative such that c_0 has bound support and is Gamma distributed with parameters ($a_\beta^{\bar{v}^*} + b_\beta^{\bar{v}^*}$, $1/\mu$), $f_{c_F}(x)$ is Gamma distributed with parameters $a_\beta^{\bar{v}^*}$ and $1/\mu$.[13] Similar conclusions are implied if $f_{c_0}(x)$ is normally distributed (with truncation so that $c_0 > 0$) with significant dispersion because the normal pdf may be applied as a limiting case of a general Gamma dispersion when the skewness is small. For low dispersion of c_0 or $c_0[(1/K) + (1/L)]^{-1}$, the Gamma approximation of f_{c_F} may be no more valid when $f_{c_F}(x)$ includes a left tail.

Stochastic migration model based on dimensionless random variables

If more than two parameters vary simultaneously, physical quantities q_i are conveniently assumed to vary as a product of a typical value or scale parameter $\overline{q_i}$ and a dimensionless random variable q_i^*. Such a strategy makes it possible to combine separately scaling factors and random contribution and thus to reduce the number of degrees of freedom of the stochastic migration model. The inverse cumulative distribution of q_i^*, denoted as $q_i^*(s_{p_i})$, is parameterized with a single shape parameter s_{p_i} because it is assumed that the shift or scale parameter is fixed. Suitable unimodal continuous distributions for q_i^* include Norm(1, s_{p_i}), logNorm(0, s_{p_i}), Weib(1, s_{p_i}), Gamma(1, s_{p_i}), and so forth. A general formulation of a full stochastic migration model is given in Eq. 8; the condition $\bar{L} \to 0$ is particularly emphasized because it corresponds to the likelihood situation encountered between FCM and food and leads to a simplified analytical expression that involves only products of continuous physical variables. For all physically consistent BC, the weak nonlinear operator $\bar{v}^*$ transforms regularly the physical space defined by $Fo^{1/2}$ into a strictly monotonous and smooth space with finite support. The final space depends regularly on values of *Bi*, *K*, and *L*

$$
\begin{aligned}
c_F(\overline{Fo},\, \overline{c_0},\, \bar{K},\, \bar{L},\, \overline{Bi},\, s_{c_0},\, s_t,\, s_D,\, s_l,\, s_K,\, s_L,\, s_{Bi}) \\
= \bar{K} \cdot \overline{c_F} \frac{c_0^*(s_{c_0})}{\dfrac{\bar{L}}{K^*(s_K)} + \dfrac{\bar{K}}{L^*(s_L)}} \\
\bar{v}^*[\overline{Fo}^{1/2} \cdot Fo^{1/2}{}^*(s_D,\, s_t,\, s_l),\, \bar{K},\, \bar{L},\, \overline{Bi},\, s_K,\, s_L,\, S_{Bi}] \\
\approx \overline{c_F} \cdot c_0^*(s_{c_0})\, L^*(s_L)\, \bar{v}^*[\overline{Fo}^{1/2} \\
\cdot Fo^{1/2}{}^*(s_D,\, s_t,\, s_l),\, \bar{K},\, \bar{L},\, \overline{Bi},\, s_K,\, s_L,\, s_{Bi}] \qquad \text{if } \bar{L} \to 0 \quad (8)
\end{aligned}
$$

where $\overline{c_F} = \bar{L} \cdot \overline{c_0}$, $\overline{Fo}^{1/2} = (\bar{D}^{1/2} \cdot \bar{t}^{1/2})/\bar{l}$, $Fo^{1/2}{}^*(s_D,\, s_t,\, s_l) = [D^*(s_D) t^*(s_t)]^{1/2}/l^*(s_l)$.

The input parameters of $\bar{v}^*$, $\overline{Fo}$, and Fo^* were replaced by their square roots because analogies between the statistics of $\bar{v}^*$ and $Fo^{1/2}$ are expected to occur when $Bi \to \infty$ (practically $Bi \geq 100$) and $Fo \to 0$ (practically $Fo < 0.6$), attributed to a possible linearization of $\bar{v}^*$ with $Fo^{1/2}$. Indeed, BC Eq. 2 degenerates into a reflecting boundary condition when $Bi \to \infty$

$$
j^* = -\frac{K}{L} \frac{\partial u|_{x^*=1}}{\partial Fo} \quad (9)
$$

where the probability of occupation at the interface $u\,|_{x^*=1}$ decays as the square root of time when $Fo \to 0$, as the standard deviation of the Brownian density u does within the FCM.

As a result, $\bar{v}^*$ increases linearly with $Fo^{1/2}$. From this point, it seems realistic to assume that $Fo^{1/2}$ and $\bar{v}^*$ have similar distributions, at least when $Fo \to 0$. For small *Fo* values, the

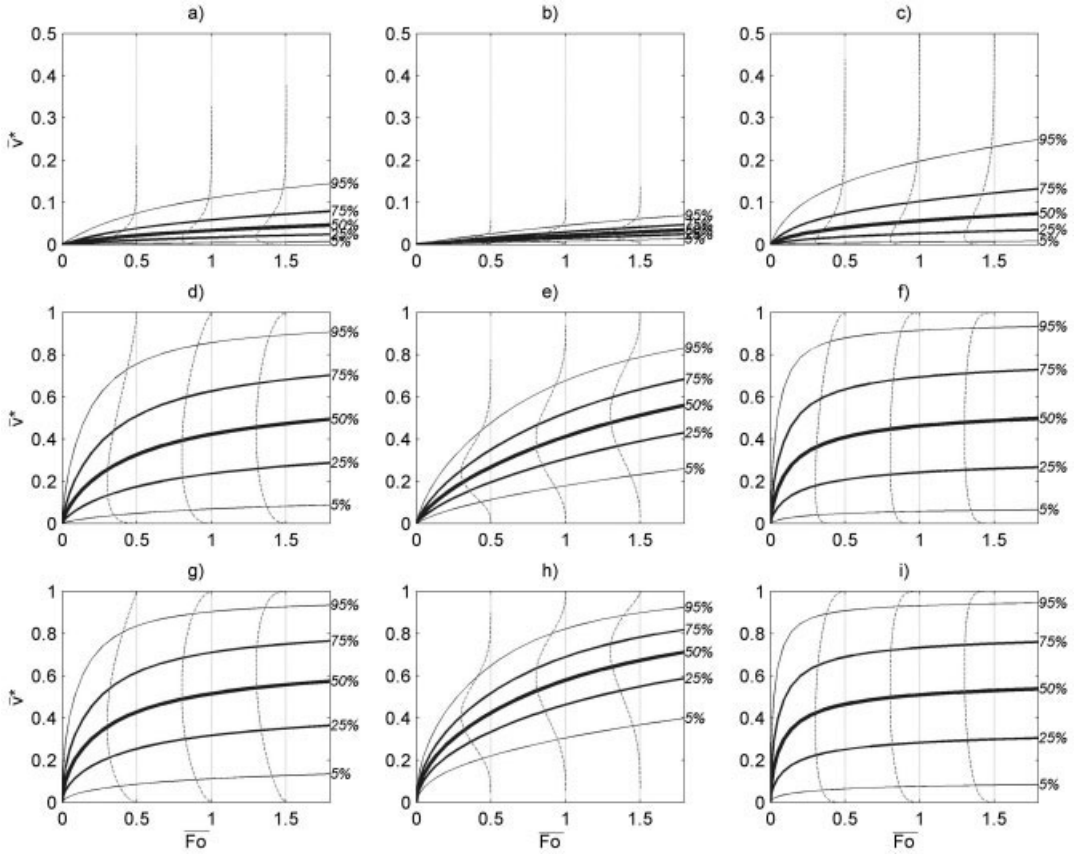

Figure 4. Percentile values of $\bar{v}^*$ for the three classes of packed food (defined in Figure 2 under M_1 assumption).

(a, d, g) class 1; (b, e, h) class 2; (c, f, i) class 3 and three typical contact conditions: (a–c) solid contact; (d–f) liquid contact; (g–i) no external resistance.

likely distribution of $Fo^{1/2}$ is therefore a generalized Beta distribution with a normalized mode < 0.5 (right-tailed or symmetric distributions). Given that truncated Gamma distributions are known to accurately approximate such Beta distributions, the latter may be used to represent any distribution of the Fo number, irrespective of the real distributions of D^*, t^*, and l^* and the value of $\overline{Fo}$ and independently on Bi values. Such an approximation ensures at least a convergence in probability of $\bar{v}^*$ for small values of Fo and $Bi > 100$. It thus seems reasonable that Gamma distributions are sufficiently generic either to fit most features of the real unbounded $Fo^{1/2}$ distributions (convergence in law) or to preserve convergence in probability for large Fo numbers, even in the case of left-tailed distributions. Indeed, convergence in probability may be preserved even in the case of a poor fit of the right-hand side of the $Fo^{1/2}$ distribution arising from the hyperexponential convergence of $\bar{v}^*$ toward the saturation value 1. Consequently, the following approximation was introduced in Eq. 8

$$Fo^{1/2*}(s_D, s_t, s_L) = \frac{D^{1/2*}(s_D)t^{1/2*}(s_t)}{l^*(s_l)} \approx \Gamma(a_\Gamma^{Fo^{1/2}}, b_\Gamma^{Fo^{1/2}}) \quad (10)$$

and $c_F(\overline{Fo}, \overline{c_0}, \bar{K}, \bar{L}, \overline{Bi}, s_{c_0}, s_t, s_D, s_l, s_K, s_L, s_{Bi})$ with 12 inputs was replaced by $c_F(\overline{Fo}, \overline{c_0}, \bar{K}, \bar{L}, \overline{Bi}, s_{c_0}, s_K, s_L, s_{Bi}, a_\Gamma^{Fo^{1/2}}, b_\Gamma^{Fo^{1/2}})$ with 11 inputs.

A more general expression of $f_{Fo^{1/2*}}(x) = pr(Fo^{1/2*} = x)$ is provided in Eqs. 11 and 12 and can be used if more accuracy is required. The starting point is that any approximation of the true distribution of $Fo^{1/2}$ may be acceptable if the distribution of $\bar{v}^*(Fo^{1/2*})$ converges to the true distribution of $\bar{v}^*$ when parameters Bi, K, and L are delta distributed. Thus, because $\bar{v}^*$ is continuous and strictly positive, the transformation $y = \bar{v}^*(x)$ is invertible so that $x = \bar{v}^*_{-1}(y)$ and can be used to transform the space of probabilities of y with respect to the space of measures of x. Because $\bar{v}^*$ is differentiable with respect to x, the transformation is given by

$$f_{Fo^{1/2*}}(x) - \beta_{(a_\beta^{\bar{v}^*}, b_\beta^{\bar{v}^*})}[\bar{v}^*(x)] \frac{\partial \bar{v}^*(x)}{\partial x} \quad (11)$$

The demonstration of Eq. 11 is straightforward by taking note of the equalities between the cumulative distributions $\int_0^x f_{Fo^{1/2*}}(\theta)d\theta = \int_0^y \beta_{(a_\beta^{\bar{v}^*}, b_\beta^{\bar{v}^*})}(v)dv$. As a result, it is verified that (1) $\bar{v}^*$ and $Fo^{1/2*}$ are distributed with respect to homothetic laws when $\bar{v}^*$ is a linear function of $Fo^{1/2*}$, (2) $f_{Fo^{1/2*}}(x)$ is left-tailed when $[\partial \bar{v}^*(Fo^{1/2*})]/\partial Fo^{1/2*} \to 0$. A simple and general prototype of $f_{Fo^{1/2*}}(x)$ from Eq. 11 can be calculated for the extreme boundary condition $Bi \to 0$ (no internal resistance to mass transfer) that imposes $\bar{v}^*$ to be an exponential function of the square root of Fo, which yields

$$\bar{v}^*(Fo^{1/2*}) = 1 - e^{-\alpha(Fo^{1/2*})^2} \quad (12)$$

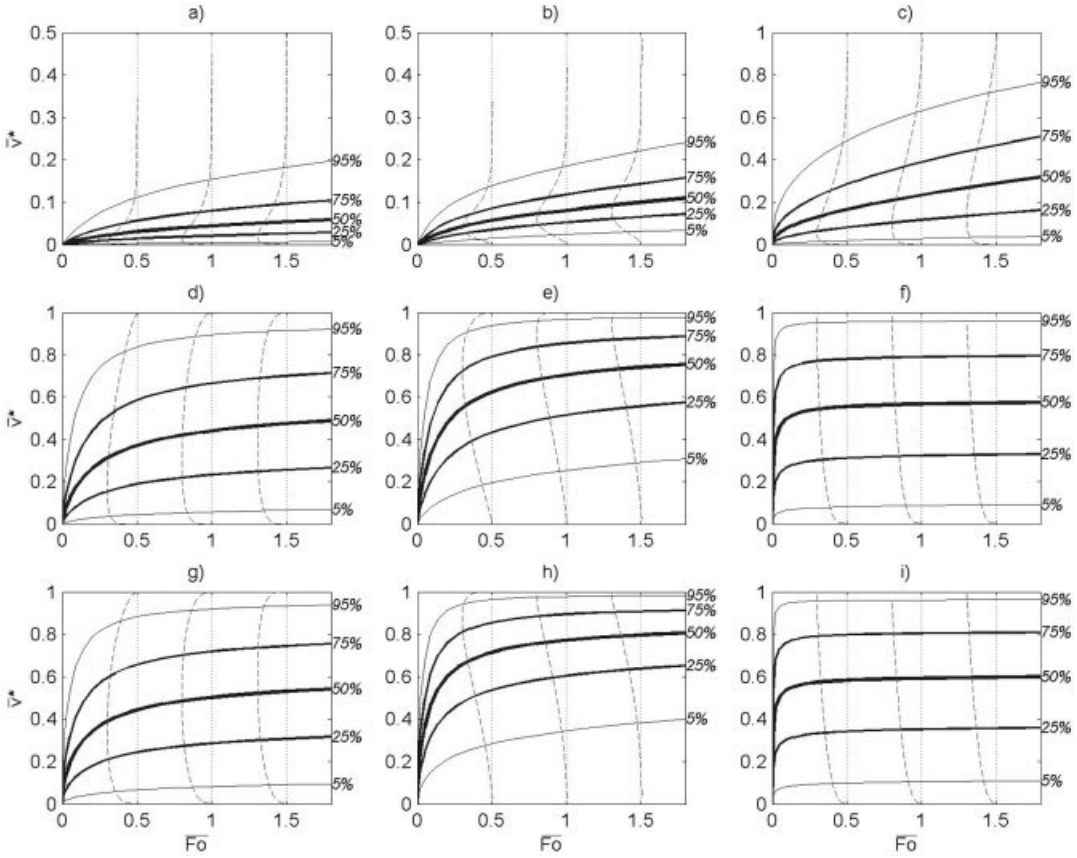

Figure 5. Percentile values of $\bar{v}^*$ for the three classes of packed food (defined in Figure 2 under M_2 assumption).

(a, d, g) class 1; (b, e, h) class 2; (c, f, i) class 3 and three typical contact conditions: (a–c) solid contact; (d–f) liquid contact; (g–i) no external resistance.

where α is an arbitrary positive constant. Because the distribution of $Fo^{1/2}*$ (square root of a dimensionless time) does not depend a priori on boundary conditions, an α value can be assigned a priori for the whole risk assessment procedure. Only parameters $a_\beta^{\bar{v}*}$, $b_\beta^{\bar{v}*}$, as they appear in Eq. 11, must be again identified when any value of the triplet $\{s_D, s_t, s_l\}$ is changed.

Numerical approximation of $f_{c_F}(x)$

The present work emphasizes the combination of efficient numerical strategies, such as fast Fourier transform (FFT) and fast regularized nonlinear *N–D* interpolation techniques, to assess the pdf of $c_F(\overline{Fo}, \overline{c_0}, \bar{K}, \bar{L}, \overline{Bi}, s_{c_0}, s_t, s_D, s_l, s_K, s_L, s_{Bi})$ for a large amount of combinations of 11 parameters that are not directly assessable by pure-force Monte Carlo techniques.

A diagram of the algorithm for the calculation of relation expressed in Eq. 8 based on the approximation expressed in Eq. 10 is presented in Figure 1 for an a priori set of continuous unimodal distributions for parameters t, D, L, K, Bi, and c_0. The algorithm is structured into four almost independent subtasks. As a result, subtasks 1, 2, and 3 may be treated or refined independently. Because subtasks 1 and 2 require iterative calculations for input parameters that vary on a specified grid, both first tasks are efficiently distributed on several processors.

(1) Identification of parameters $(a_\Gamma^{Fo^{1/2}}, b_\Gamma^{Fo^{1/2}})$ that approximate $Fo^{1/2}*(s_D, s_t, s_L)$ according to Eq. 10 for any triplet $\{s_D, s_t, s_L\}$ belonging to a prescribed closed-frame space.

(2) For a given set of parameters $\overline{Bi}$, $\bar{K}$, $\bar{L}$ with $s_{Bi} = s_K = s_L = 0$, the values of $(a_\beta^{\bar{v}*}, b_\beta^{\bar{v}*})$ are identified from $\bar{v}*(\overline{Fo}^{1/2}, a_\Gamma^{Fo^{1/2}}, b_\Gamma^{Fo^{1/2}})$ for any triplet $\{\overline{Fo}^{1/2}, a_\Gamma^{Fo^{1/2}}, b_\Gamma^{Fo^{1/2}}\}$ belonging to a frame space that includes realistic values of $\overline{Fo}^{1/2}$ and the joint interval of $a_\Gamma^{Fo^{1/2}} \times b_\Gamma^{Fo^{1/2}}$ inferred in subtask 1.

(3) The joint pdf of $\bar{v}*$ corresponding to $\beta[a_\beta^{\bar{v}*}(a_\Gamma^{Fo^{1/2}}, b_\Gamma^{Fo^{1/2}}, s_K, s_L, s_{Bi}), b_\beta^{\bar{v}*}(a_\Gamma^{Fo^{1/2}}, b_\Gamma^{Fo^{1/2}}, s_K, s_L, s_{Bi})]_{\overline{Fo},\bar{K},\bar{L},\overline{Bi}}$ is calculated as a mixture of Beta distributions. The N-variate of the $\bar{v}*$ pdf with respect to each input random variable ($Fo*$, $K*$, $L*$, $Bi*$) is thus treated as the N tensor-product of its individual variations. Because $\bar{v}*$ varies continuously with K, L, and Bi, values of s_K, s_L, and s_{Bi} may be interpreted indifferently either as shape parameters of K, L, and Bi distributions, respectively, or as confidence intervals on $\bar{K}$, $\bar{L}$, and $\overline{Bi}$values, respectively. When $s_K = s_L = s_{Bi} = 0$ (currently the most practical situation), an efficient estimation of the Beta distribution is indifferently calculated (1) by projecting the measures of the calculated $f_{Fo^{1/2}*}(x)$ onto an approximation space of $\bar{v}*$ (such as that based on piecewise cubic Hermite polynomials) or (2) by the reciprocal of Eq. 11

$$\beta_{(a_\beta^{\bar{v}*}, b_\beta^{\bar{v}*})}(y) = f_{Fo^{1/2}*}[\bar{v}*_{-1}(y)] \frac{\partial \bar{v}*_{-1}(y)}{\partial y} \tag{13}$$

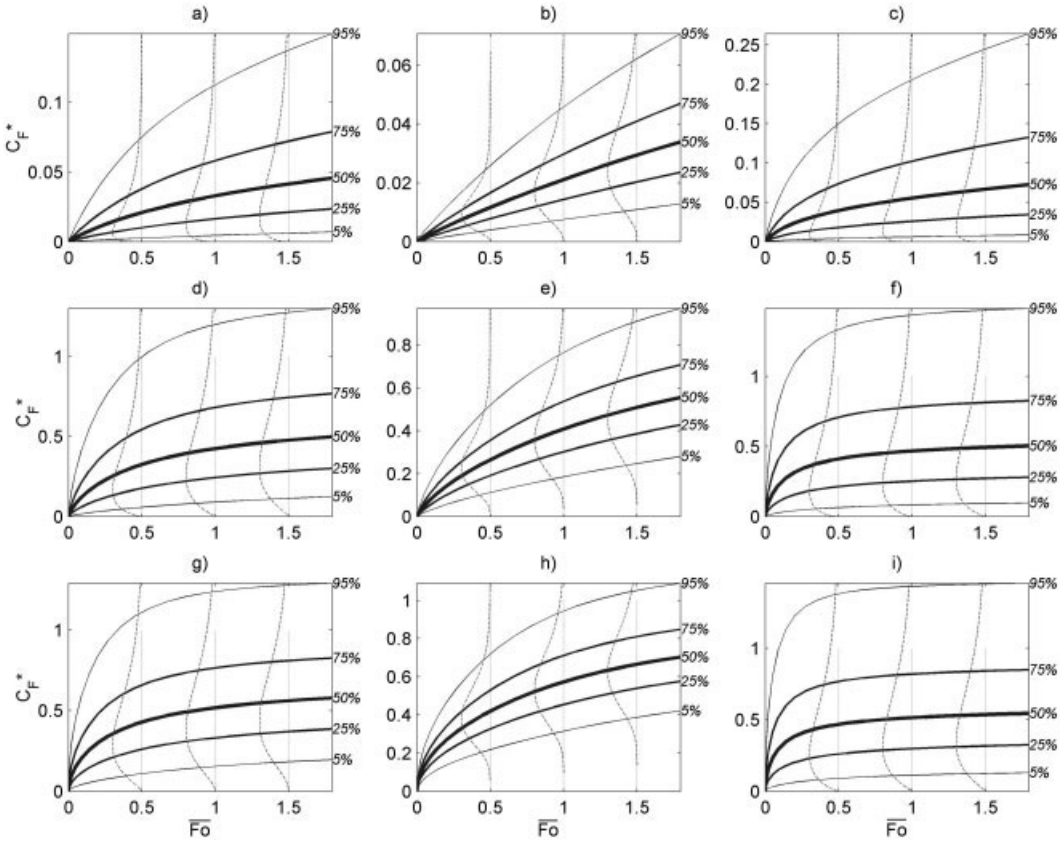

Figure 6. Percentile values of c_F for the three classes of packed food (based on results presented in Figure 4).

(a, d, g) class 1; (b, e, h) class 2; (c, f, i) class 3 and three typical contact conditions: (a–c) solid contact; (d–f) liquid contact; (g–i) no external resistance.

(4) The pdf of

$$c_F(\cdots) = \bar{K} \cdot \overline{c_F} \frac{c_0^*(s_{c_0})}{\dfrac{\bar{L}}{K^*(s_K)} + \dfrac{\bar{K}}{L^*(s_L)}} \bar{v}^*(\cdots)$$

is finally calculated as the pdf of a product of continuous random variables.

The pdf of the product of n variables, which appears in subtasks 1 and 4, is iteratively calculated from the convolution of two log-transformed absolutely positive variables, X and Y, where the product $X \cdot Y$ is written $e^{\ln X + \ln Y}$. After normalization, variables $\ln X$ and $\ln Y$ are uniformly sampled on a common interval so that the number of samples is a power of 2 and the convolution may be performed as the product of the FFTs of the PDFs $\ln X$ and $\ln Y$, respectively. A similar strategy, based on convolution, is applied to assess $\bar{L}K^*(s_K)^{-1} + \bar{K}L^*(s_L)^{-1}$ (see subtask 4).

Because $\bar{v}^*$ is infinitely differentiable with respect to each input, the $\bar{v}^*$ transformation is interpreted as a local interpolation operator based on multivariate cubic splines. As a result, $\bar{v}^*$ values are interpolated within (1) an N-dimension Cartesian grid that meshes the N–D space of parameters (including between 20^N and 40^N nodes according to the value of N), and (2) the precalculated values at the nodes of the grid. All grids are irregular so as to locally update the grid steps according to the Hessian of $\bar{v}^*$. The values at the nodes are calculated from the numerical resolution of Eqs. 1 and 2 with $u(x, Fo = 0) = 1$ as the initial condition with a finite-element technique based on 50 quadratic Lagrangian elements. Implicit numerical differential formula up to order 3 are used for time integration to preserve an absolute accuracy of 10^{-6} during the whole process of time marching.

The identification of Beta and Gamma parameters from calculated distribution is based on a mean-square approximation of the corresponding theoretical pdf. The minimization is reliably performed using the Nelder–Mead algorithm with an initial guess based on analytical estimates.

Risk Scenarios Based on Classes of Packed Food Products

Definition of classes and constitutive hypotheses

The proposed dimensionless formulation makes it possible to hypothesize that packed food articles may be classified according to invariant criteria based on the shape of the distributions of typical quantities: $D/\bar{D}$, $t/\bar{t}$, $l/\bar{l}$. Theses distributions provide relative estimates of both variability and uncertainty from the magnitude of pertinent quantities in migration risk. In this work, the type and shape of their distribution were pragmatically defined from expert opinions and all quantities $\bar{q}$ were related to likely values in the sense of likely scenarios, as experts would do it.

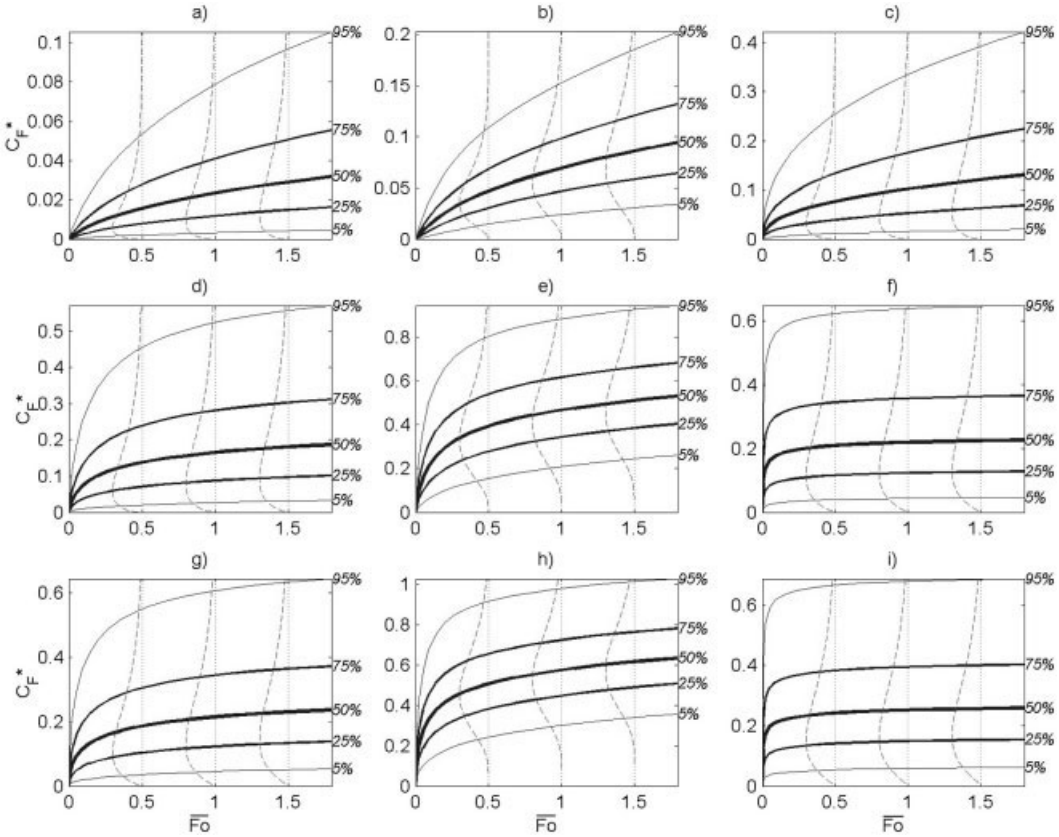

Figure 7. Percentile values of c_F for the three classes of packed food (based on results presented in Figure 5).

(a, d, g) class 1; (b, e, h) class 2; (c, f, i) class 3 and three typical contact conditions: (a–c) solid contact; (d–f) liquid contact; (g–i) no external resistance.

$D/\bar{D}$ was thus assumed to be log-normally distributed with parameters log $N(0, s_D)$ because D values in packaging materials range over more than 10 decades according to more or less understood criteria (polymer type, volume and geometry of the migrant, temperature, concentration in plasticizer, process conditions, etc.). Two hypothetical contamination conditions, designated M_1 and M_2, were considered:

- M_1: contamination by a specific migrant with a well-known $\bar{D}$ value (such as migration of styrene from PS packaging into yogurt).
- M_2: contamination by a pool of migrants with similar chemical structure (such as plasticizers from PVC films or antioxidants from polyolefins) or by a single migrant with a poorly known $\bar{D}$ value.

Both extreme cases provide insight in the uncertainty of the model results according to the most variable or unknown quantity D. s_D levels of 0.15 and 0.5 were chosen for M_1 and M_2, respectively.

For a similar packaging type (such as films, bottles, tubes, bags, etc.), $l/\bar{l}$, on the contrary, was expected to vary symmetrically and in a narrower range following a normal distribution of parameters $N(1, s_l)$. Two s_l levels were chosen: 0.01 (almost delta distributed) and 0.15.

In the absence of dedicated studies on the contact time of packaging with food during transport, retail and domestic storage, a generic Weibull distribution was applied for $t/\bar{t}$. The Weibull distribution of parameter $W(1, s_t)$ was chosen because it is always positive, is easily scalable, and belongs to exponential distributions that are generally used to describe complex waiting time distributions. It must be emphasized that distributions with semi-infinite support (that is, nontruncated) cannot account for any restriction attributed to a sell-by date or eat-by date (t_{max}). To be realistic, chosen $\bar{t}$ must therefore be chosen so that $\bar{t} < t_{\max}$. Two extreme shape were tested by setting $s_t = 1.2$ and $s_t = 3$. When $s_t \to 1^+$, $t/\bar{t}$ is highly dissymmetric with a left mode, whereas it is almost symmetric when $s_t \to \infty$.

The hypotheses for the definition of three classes of packed food products under two migration conditions, M_1 and M_2, are summarized in Figure 2. Distributions of the contamination respectively to the previous classes were investigated for 3 typical boundary conditions or contact type conditions, called BC_1, BC_2, and BC_3, and detailed in Table 1. BC_1 and BC_3 correspond to two extreme cases, respectively: (1) an almost solid food ($\overline{Bi} \to 1$, a very significant external resistance to migration) with a sparingly soluble migrant ($\bar{K} < 1$, a significant thermodynamic resistance to migration), (2) a liquid food with neither a significant external resistance to mass transfer ($\overline{Bi} \gg 1$, such as stirred liquid food) nor a hydrodynamic resistance ($\bar{K} = 1$, good migrant solubility). An $\bar{L}$ of 2×10^{-2} is found, for example, for a yogurt container. Boundary condition BC_2 is intermediate and more likely for semiliquid or nonstirred liquid food products with intermediate migrant solubility in food. The effects of the selected boundary conditions

Table 2. Distributions of Random Variables and Corresponding Ranges of Parameters That Were Explored

Variable	Distribution	Distribution Parameters	Range
$\overline{Fo}$	δ	$\overline{Fo}$	10^{-6}–50
$Fo^{*1/2}$	Gamma(a_Γ, b_Γ)	a_Γ, b_Γ	Figure 9
D^*	$\log_{10}$Norm(1, s_D)	s_D	0–0.5
t^*	Weib(1, s_t)	s_t	1–6
l^*	Norm(0, s_l)	s_l	0–0.3
$\bar{v}^*$	Beta($a_\beta^{\bar{v}^*}$, $b_\beta^{\bar{v}^*}$)	$a_\beta^{\bar{v}^*}$, $b_\beta^{\bar{v}^*}$	Figures 10, 11, 12

on dimensionless migration kinetics and on $\bar{v}^*$ distribution for a given Fo distribution are illustrated in Figure 3. One notes the transition of the $\bar{v}^*$ distribution with a left mode to a right one for an identical Fo distribution when BC_2 is changed to BC_3.

Distributions of $\bar{v}^*$

The percentile values of $\bar{v}^*$ for the three classes of packed food products and the three tested boundary conditions are presented in Figures 4 and 5 vs. $\overline{Fo}$ to migration conditions M_1 and M_2, respectively. Continuous $\bar{v}^*$ distributions are also plotted for $\overline{Fo}$ values 0.5, 1, and 2, which illustrate several typical shapes of Beta distribution of $\bar{v}^*$ from a left J-shape (Figures 4a, 5a, and 5b) to a right one (Figure 5e) by a bell shape (Figures 4e and 4h) and a reverse U-shape (Figures 4g, 4i, 5d, and 5g).

For $\overline{Fo}$ ranges between 0 and 2, the percentile values exhibited a monotonous increase with $\overline{Fo}$ as do migration kinetics presented in Figure 3. The dispersion in $\bar{v}^*$ values for an identical $\overline{Fo}$ was higher than both the dispersion of Fo^* and the value of $\overline{Fo}$ was higher. As a result, class 3 and migration condition M_2 that included the highest variability apparently led to rapid increases of percentile values up to different plateau values (see Figures 5f–i). These plateaus, with values different from 1, have no physical meaning because they are not related to any thermodynamic equilibrium. It was verified that they were not true asymptotes and that all critical values converged toward 1 when $\overline{Fo} \to \infty$. Asymptotic behavior occurs when both parameters $a_\beta^{\bar{v}^*}$ and $b_\beta^{\bar{v}^*}$ do not change significantly with $\overline{Fo}$, that is, when $\overline{Fo}$ (here in the range between 0 and 2) is small compared to the amplitude of the variation of Fo^*.

In detail, the effect of boundary conditions is higher than the effect of class of packed food products. As it is illustrated in Figure 3, boundary conditions control how a given Fo distribution is transformed into a Beta distribution of $\bar{v}^*$. Thus, a solid contact with food for dimensionless contact times $\overline{Fo} < 2$, combined with a medium dispersion leads to a quasi-symmetric narrow beta distribution of $\bar{v}^*$ with a mode < 0.3. For similar dimensionless contact times, semiliquid or liquid contacts lead by contrast to all possible shapes and mode positions for the distribution of $\bar{v}^*$. From these observations when $\overline{Fo} > 1$, the classification of packed food should be supported mainly by criteria on conditions of contact between packaging and food rather than by statistical criteria since the effects of both variability or uncertainty are not significant for given acceptable risk $1 - pr$ (such as $pr = 95\%$, also noted 95th percentile value).

When $\overline{Fo} \leq 1$, a risk analysis independent of the shape of the Fo distribution and only based on the type of contact would not be sufficient to assess accurately an upper limit of the migration risk. For $\overline{Fo} = 0.1$, the 95% percentile value of $\bar{v}^*$ is 0.1 in the case of packed food products of class 2 under the migration condition M_1 and BC_3 (Figure 4h), whereas it is >0.7 for packed food products of class 3 under similar migration conditions (Figure 4i). In the same way, changing a migration condition from the M_2 case to the M_1 one—resulting, for instance, from a reduction in the D uncertainty—decreases the 95th percentile value of $\bar{v}^*$ from 0.5 (Figure 5h) 0.1 (Figure 4h).

Distributions of c_F

Figures 6 and 7 plot the percentile values of c_F vs. $\overline{Fo}$, with respect to $\bar{v}^*$ values plotted in Figures 4 and 5. They assume a dimensionless initial concentration in the packaging of $\overline{c_0} = 1$ and a normal distribution of c_0^* with parameters $N(1, s_{c_0} = 0.15)$. In the calculations, the normal distribution was truncated so that c_0 was always positive. Because $\bar{v}_\infty$ was almost similar for all three classes (see Table 1), the percentile values of c_F are comparable between classes.

Calculated continuous c_F distributions plotted for $\overline{Fo} = 0.5$, 1, and 2 confirm that distributions of c_f and $\bar{v}^*$ have strong similarities, in spite of changes in scale values. When the dispersion of $\bar{v}^*$ is high (see Figures 5g–i), the final c_f distribution (see Figures 7g–i) has a similar dispersion with a mode displaced in the left direction. By contrast, when the dispersion of $\bar{v}^*$ is low (see Figures 4a and 4b), the final c_f distribution has a higher dispersion and a similar shape (see Figures 6a and 6b). All plotted distributions were conveniently approximated by gamma distributions. As a result Gamma distributions may be proposed as a general distribution for the contamination of packed food when it is assumed that $c_0\bar{v}_\infty$ is almost normally

Table 3. Decision Tree for Choosing Boundary Conditions That Do Not Belong to Tested Conditions of $\overline{Bi}$, $\bar{K}$, and $\bar{L}$ Values

Condition	Relevance	Suitable Approximation	Consistency
$\overline{Bi}$			
$\overline{Bi} < 1$	Unlikely	BC_1	Overestimation
$1 \leq \overline{Bi} \leq 10^3$	Common	BC_1, BC_2, BC_3	Acceptable
$\overline{Bi} > 10^3$	Low probable	BC_3	No significant underestimation
$\bar{K}$			
$\bar{K} > \bar{L}$	Common	BC_1, BC_2, BC_3	Depend mainly on the $\overline{Bi}$ value
$\bar{K} \approx \bar{L}$ or $\bar{K} < \bar{L}$ with $\bar{L} < 3/\overline{Bi}$	Probable	BC_3	Overestimation
$\bar{K} \approx \bar{L}$ or $\bar{K} < \bar{L}$ with $\bar{L} > 3/\overline{Bi}$	Uncommon	BC_3 (instantaneous equilibrium)	Underestimation (overestimation)
$\bar{L}$			
$\bar{L} \ll \bar{K}$	Common	BC_3	Slight overestimation
$\bar{L} < 3/\overline{Bi}$	Common	BC_3	Overestimation (smaller if $\overline{Bi}$ is large)
$\bar{L} > 3/\overline{Bi}$	Uncommon	BC_3 (instantaneous equilibrium)	Underestimation (overestimation)

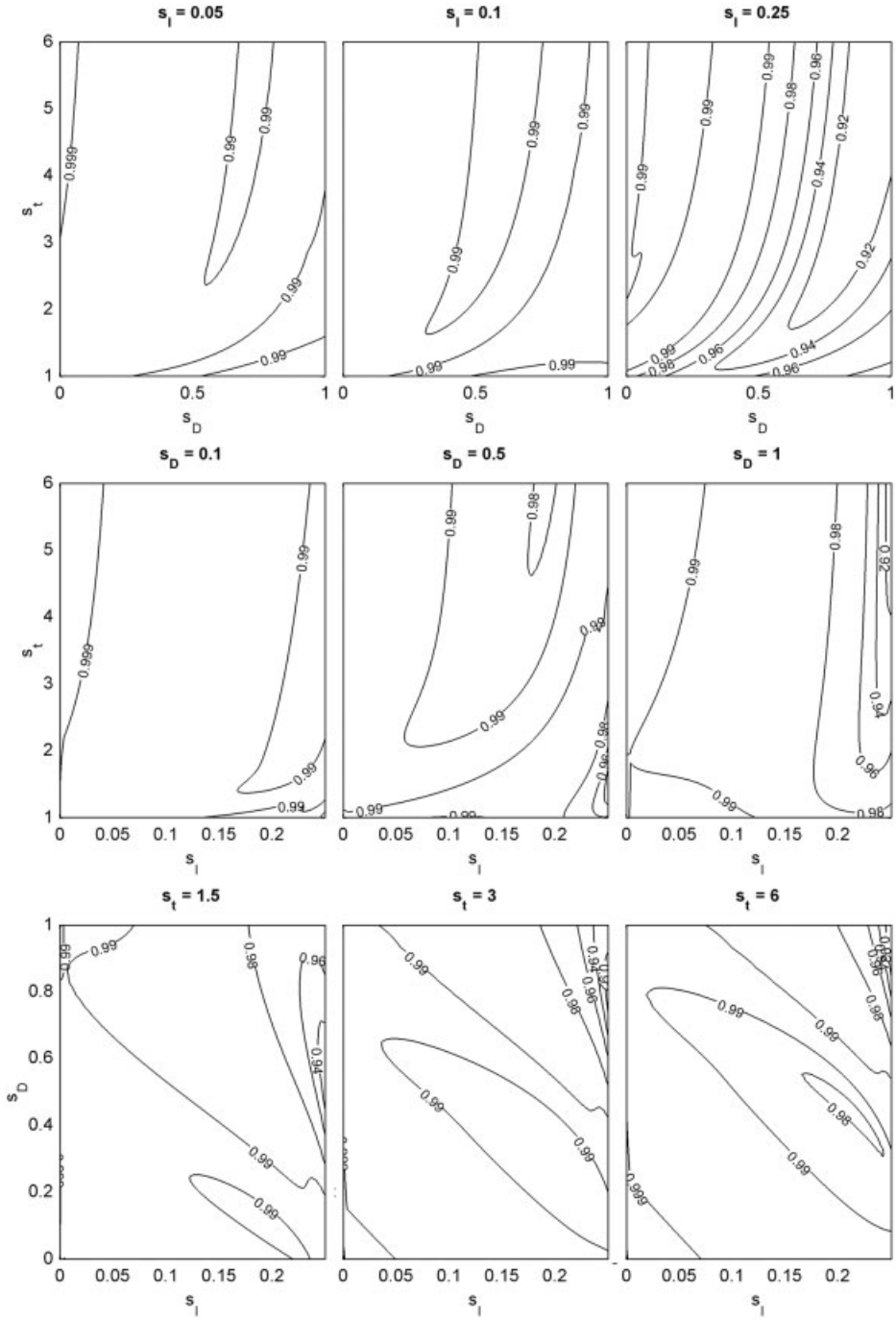

Figure 8. Determination coefficient (r^2) related to the approximation of the pdf of $Fo^*(s_D, s_t, s_l)^{1/2}$ by a gamma distribution.

distributed or obey any law with a distribution with a tail longer than that of the normal distribution (such as log-normal, Gamma, etc.). An attractive characteristic of the Gamma distribution to be used for assessment of exposure to substances from packaging is that the sum of n random variables with a Gamma(α, β) distribution is Gamma($n\cdot\alpha$, β) distributed. However, it must be emphasized that, because the Gamma distribution has no upper limit, some values may be not physically realistic as a result of either mass balance or thermodynamic constraints. Consequently, and as a result of similarity between the distributions of c_F and $\bar{v}^*$, the BetaPert or generalized Beta distributions may be proposed as alternatives when Gamma distributions do not seem suitable and when the maximum realistic value is known.

Abacuses of Parameters of the $\bar{v}^*$ Distribution: $a_\beta^{\bar{v}^*}$, $b_\beta^{\bar{v}^*}$

Previous c_F and $\bar{v}^*$ distributions based on risk scenarios provide confidence intervals and may be easily applied to make

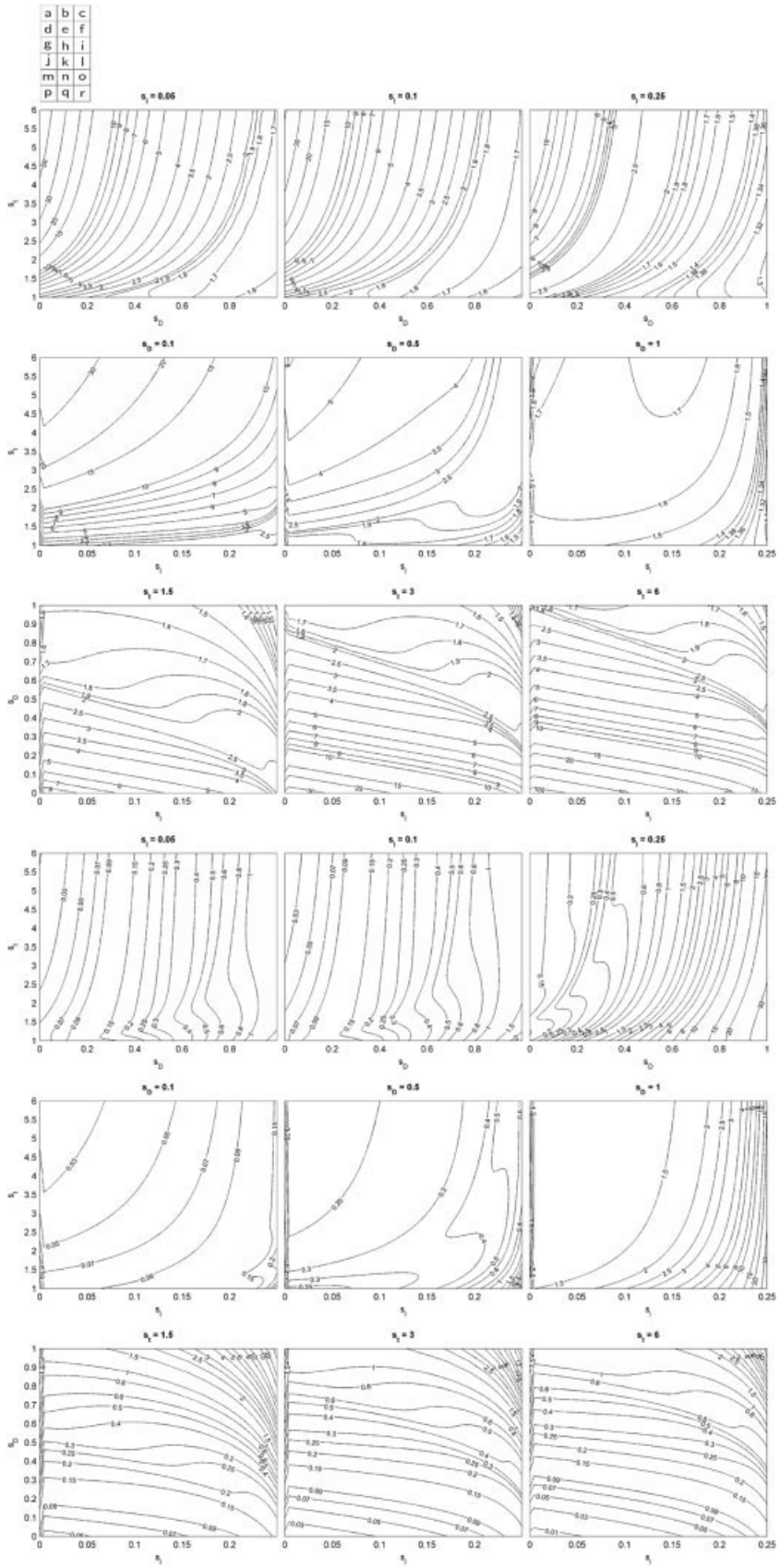

Figure 9. Fitted parameters a_Γ and b_Γ that approximate the pdf of $Fo^*(s_D, s_t, s_l)^{1/2}$ by $\Gamma(a_\Gamma, b_\Gamma)$.

(a–i) a_Γ isovalues; (j–r) b_Γ isovalues.

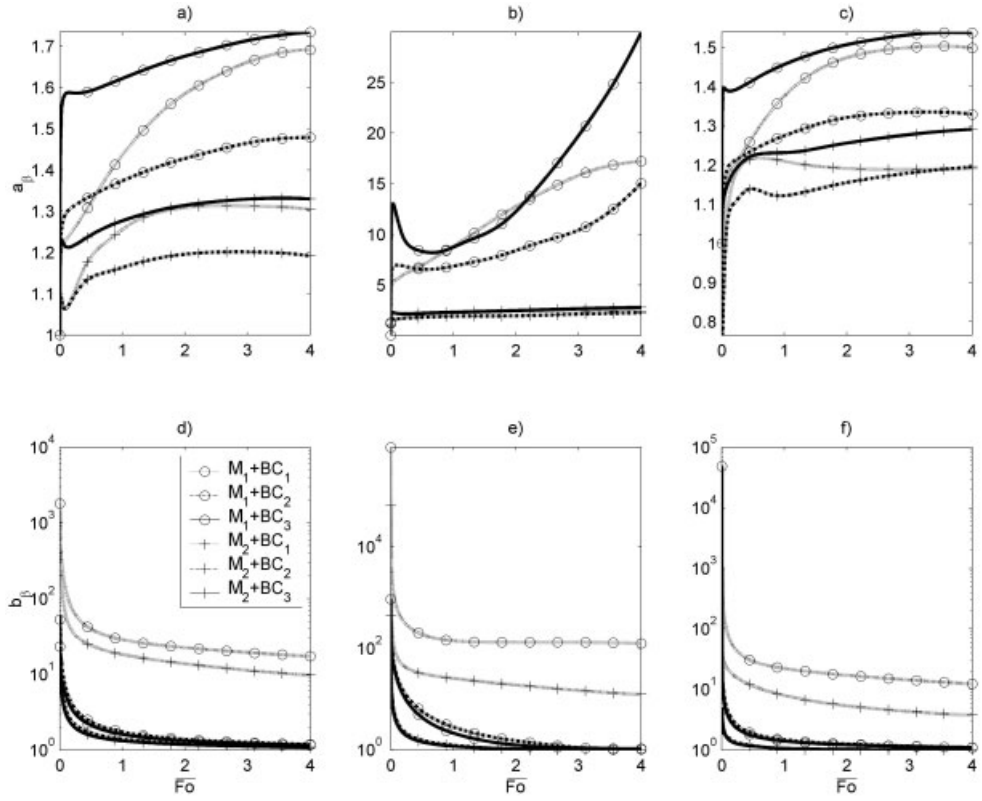

Figure 10. Variations of a_β (a–c) and b_β (d–f) values for the three classes of food with $\overline{Fo}$, respectively, to : (a, d) class 1, (b, e) class 2, (c, f) class 3.

point estimates or to classify substances, packaging, applications according to a risk of contamination, or migration beyond a given threshold. They are expected to be very useful for experts of food and packaging sectors but also for control and monitoring authorities. However, they afford no prediction of respective contributions of uncertainty and variability because both concepts are mixed in the previous concept of class. The following part provides data analysis abacuses that may be used to generalize the previous approach for any realistic values (1) of scale parameters: $\bar{D}$, $\bar{t}$, and $\bar{l}$ combined as $\overline{Fo} = \bar{D}\cdot\bar{t}/\bar{l}^2$ in the range 10^{-6} and 50; and (2) of shape parameters s_D, s_t, and s_l. The explored domain is detailed in Table 2. Sensitivity analysis around a likelihood $\overline{Fo}$ value may thus be performed by changing any of the values of s_D, s_t, and s_l and by comparing the effects with a reference condition.

For brevity, only $\bar{v}^*$ results for previous BC_1, BC_2, and BC_3 are presented. A discussion regarding other boundary/contact conditions is provided for convenience in Table 3. BC_1 and BC_3, with *Bi* numbers ranging between 1 and 10^3, are expected to include the whole range of *Bi* realistic values. Values of $K < 0.1$ were not considered because these values did not significantly change the dimensionless migration kinetics $\bar{v}^* = f(Fo)$, whereas $\bar{K} \gg \bar{L}$ ($\bar{L}$ values are assumed to be small in the case of packaging materials). When the previous conditions are not fulfilled (that is, $\bar{K} \approx \bar{L}$ or $\bar{K} < \bar{L}$), the curve obtained for $\bar{K} = 1$ and similar L and Bi values may be used as a pessimistic scenario while $\bar{L} < 3/\overline{Bi}$. In very unlikely scenarios where $\bar{K} \ll \bar{L}$ (such as high sparingly soluble substance in food) and $\bar{L} > 3/\overline{Bi}$ (such as thick packaging material and/or continuously stirred liquid food), $\bar{v}^*$ is increasing with *Fo* more rapidly than during BC_3. As a result, BC_3 may underestimate the true dimensionless migration kinetic and a best approximation may be obtained by neglecting kinetic effects and by assuming an instantaneous thermodynamic equilibrium ($\bar{v}^* = 1$).

Whatever the boundary conditions, $\bar{v}_\infty$ must be approximated by the most likely values of $\bar{K}$ and $\bar{L}$. Only if $\bar{K} \gg \bar{L}$, may $\bar{v}_\infty$ be approximated by $\bar{L}$.

With respect to the diagram given in Figure 1, Figures 8 and 9 provide parameters that approximate the distribution of $Fo^{*1/2}$ by a Gamma distribution in relation to the value of shape parameters. Figures 10, 11, and 12 plot the parameters of the Beta distribution of $\bar{v}^*$ in relation to $\overline{Fo}$ and the parameters of the approximated distribution of $Fo^{*1/2}$ given in Figure 9. Given that all abacuses are function of three inputs, only orthogonal planes with respect to given values of each input are depicted. Each surface response is represented as contour plots and combined with filled surfaces that were darkened according to the log of the response.

Approximation of the distribution of $Fo^*(s_D, s_t, s_l)^{1/2}$ by a Gamma distribution $\Gamma(a_\Gamma^{Fo^{1/2}}, b_\Gamma^{Fo^{1/2}})$

As previously explained, the approximation of the true distribution of $Fo^{*1/2}$ by a continuous known distribution was not a necessary step, which was compelled by any particular calculation limit, but was proposed as a suitable simplification to keep the number of required abacuses as low as possible. Figure 8 illustrates the relevance of the proposed Gamma

[$\Gamma(a_\Gamma, b_\Gamma)$] approximation by plotting the determination coefficients for all tested conditions. The true distributions of $Fo^{*1/2}$ and their approximations were calculated for 6×10^4 combinations of the shape parameters s_D, s_t, and s_l distributed on a Latin cube. For each combination of the three parameters, the least-square identification of procedure was based on 3×10^3 points that equisampled the space of the calculated cumulative distribution function.

Determination coefficients demonstrate that the Gamma distribution conveniently fits the true distribution of $Fo^{*1/2}$ for the whole range of examined combinations of shape parameters (see Table 2). In most cases, determination coefficients were >0.98. Lower values, down to 0.9, were obtained when wide distributions of D^*, t^*, and l^* were combined, respectively, for $s_D > 0.4$, $s_t < 1.2$, and $s_l > 0.2$. These situations corresponded in particular to fitted Gamma distributions with longer tails than the true ones. Because no values < 0.9 were obtained and because tail values for large $Fo^{1/2}$ values lead to similar migration rates (that is, values close to 1), the Gamma approximation was assumed acceptable and without significant effects on the contamination risk assessment.

Corresponding a_Γ and b_Γ values, plotted in Figure 9, ranged between 1.2 and 30 and between 10^{-3} and 10, respectively. According to the chosen distribution laws and ranges of shape parameters, s_D had a substantial influence on both a_Γ and b_Γ parameters, and s_t exerted a greater influence than s_l when s_D is low. As a result, isocontours were almost perpendicular to the s_D axis.

Typical values of $a_\beta^{\bar{\nu}^*}$, $b_\beta^{\bar{\nu}^*}$ for the three classes of packed food products

Figure 10 plots the variation of parameters $a_\beta^{\bar{\nu}^*}$, $b_\beta^{\bar{\nu}^*}$ vs. $\overline{Fo}$ for the three classes of packed foods. The parameter $b_\beta^{\bar{\nu}^*}$ decreases continuously with $\overline{Fo}$ from infinite toward 1 when $\overline{Fo} \to \infty$, whereas the parameter $a_\beta^{\bar{\nu}^*}$ varies nonmonotonously and nontrivially with respect to the shape of $\bar{\nu}^*$. Values of $a_\beta^{\bar{\nu}^*} < 1$ observed for class 3 and $\overline{Fo}$ values close to 0 correspond to the exponential distribution, whereas values of $a_\beta^{\bar{\nu}^*} > 1$ correspond to a mode significantly different from zero. If $b_\beta^{\bar{\nu}^*}$ is higher than $a_\beta^{\bar{\nu}^*}$, the distribution is right-tailed and, reciprocally, it is left-tailed if $a_\beta^{\bar{\nu}^*}$ is higher than $b_\beta^{\bar{\nu}^*}$. As a result of higher $b_\beta^{\bar{\nu}^*}/a_\beta^{\bar{\nu}^*}$ ratios for M_2 than those for M_1 conditions, the distribution is more asymmetric in the M_2 case.

Parameters $a_\beta^{\bar{\nu}^*}$, $b_\beta^{\bar{\nu}^*}$ of the distribution of $\bar{\nu}^*$ according to $\overline{Fo}$, a_Γ, b_Γ

Figures 11, 12, and 13 plot isovalues of $a_\beta^{\bar{\nu}^*}$, $b_\beta^{\bar{\nu}^*}$ and the corresponding 50th percentile value, denoted as x_{50}, vs. $\overline{Fo}^{1/2}$, a_Γ, and b_Γ, respectively, for boundary conditions BC_1, BC_2, and BC_3. For each output and boundary condition, nine typical planes including the whole practical domain $Fo = 10^{-6}$–10^2, $a_\Gamma = 1.3$–2, and $b_\Gamma = 10^{-3}$–2 are depicted. By decreasing the order of significance, all three parameters, $\overline{Fo}^{1/2}$, a_Γ, and b_Γ, control the values of $a_\beta^{\bar{\nu}^*}$ and $b_\beta^{\bar{\nu}^*}$. x_{50} increases monotonously with all three parameters and all the more sharply as the external resistance is decreasing (that is, in the order BC_1, BC_2, BC_3).

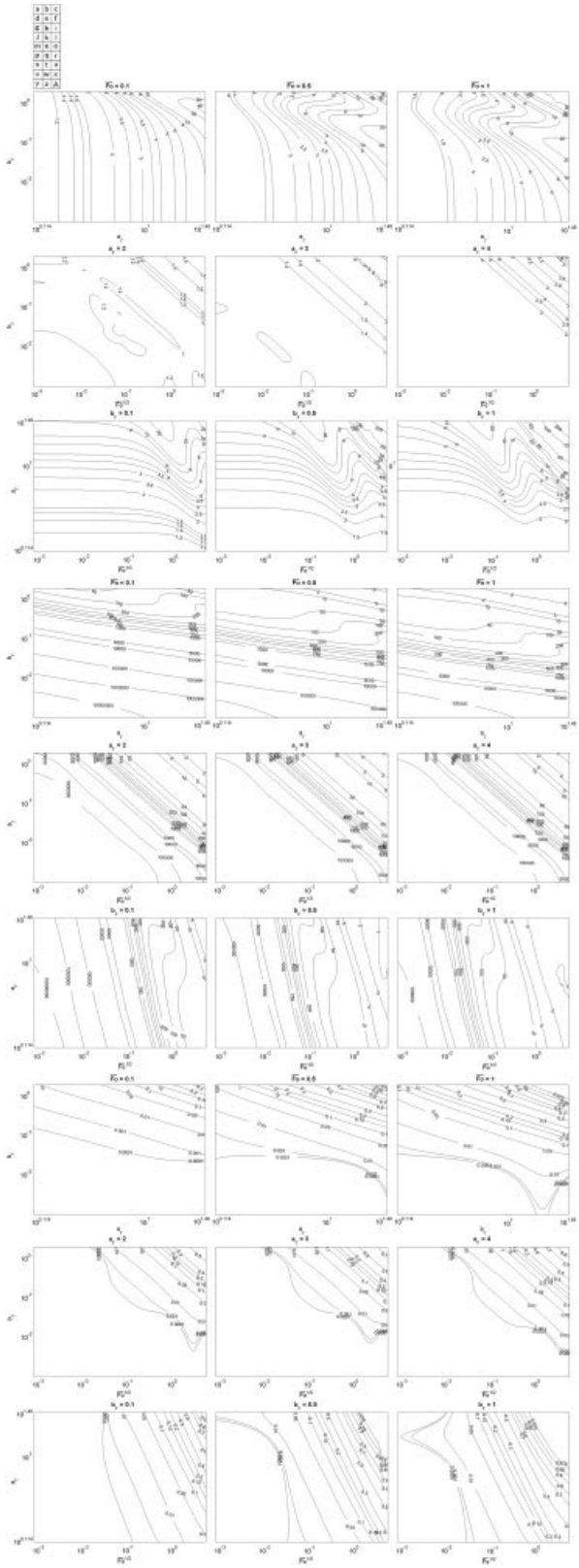

Figure 11. Fitted parameters a_β, b_β, and corresponding 50th percentile values x_{50} that approximate the pdf of $\bar{\nu}^*(\overline{Fo}, a_\Gamma, b_\Gamma)$ by $Beta(a_\beta, b_\beta)$ for the boundary condition BC_1.

(a–i) a_β isovalues, (j–r) b_β isovalues, (s–A) x_{50} values.

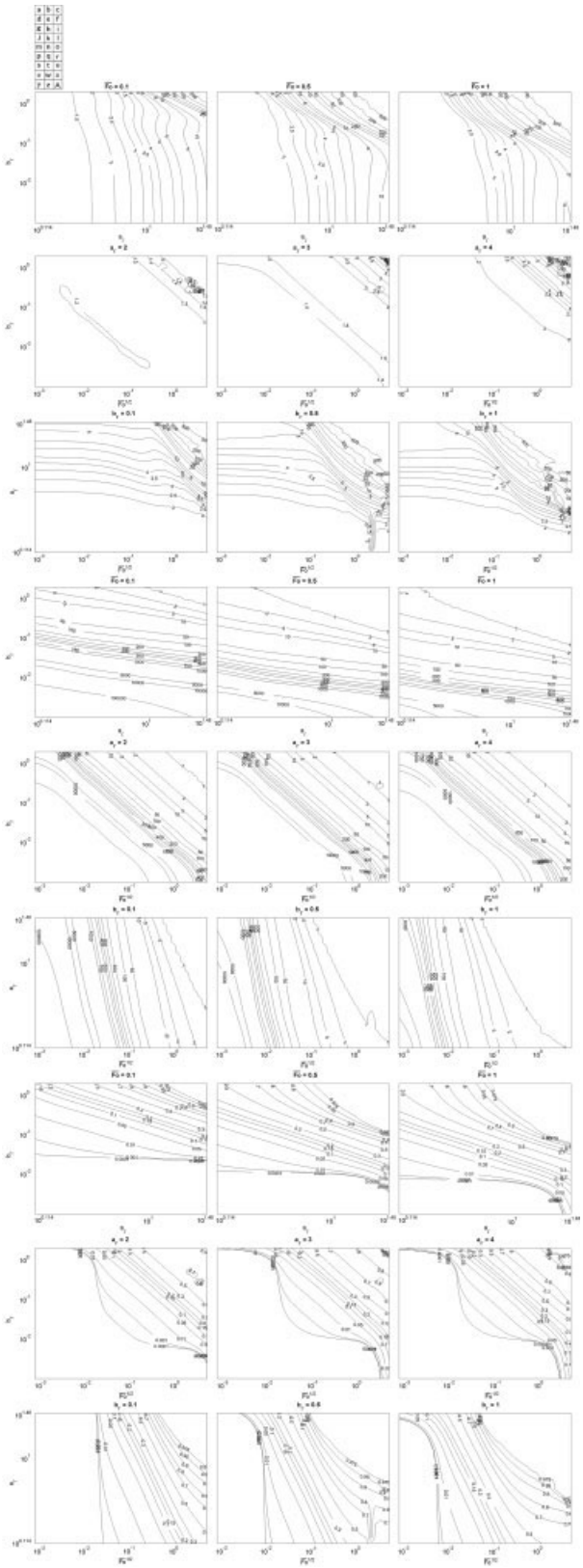

Figure 12. Fitted parameters a_β, b_β, and corresponding 50th percentile values x_{50} that approximate the pdf of $\bar{v}^*(\overline{Fo}, a_\Gamma, b_\Gamma)$ by $Beta(a_\beta, b_\beta)$ for the boundary condition BC_2.

(a–i) a_β isovalues, (j–r) b_β isovalues, (s–A) x_{50} values.

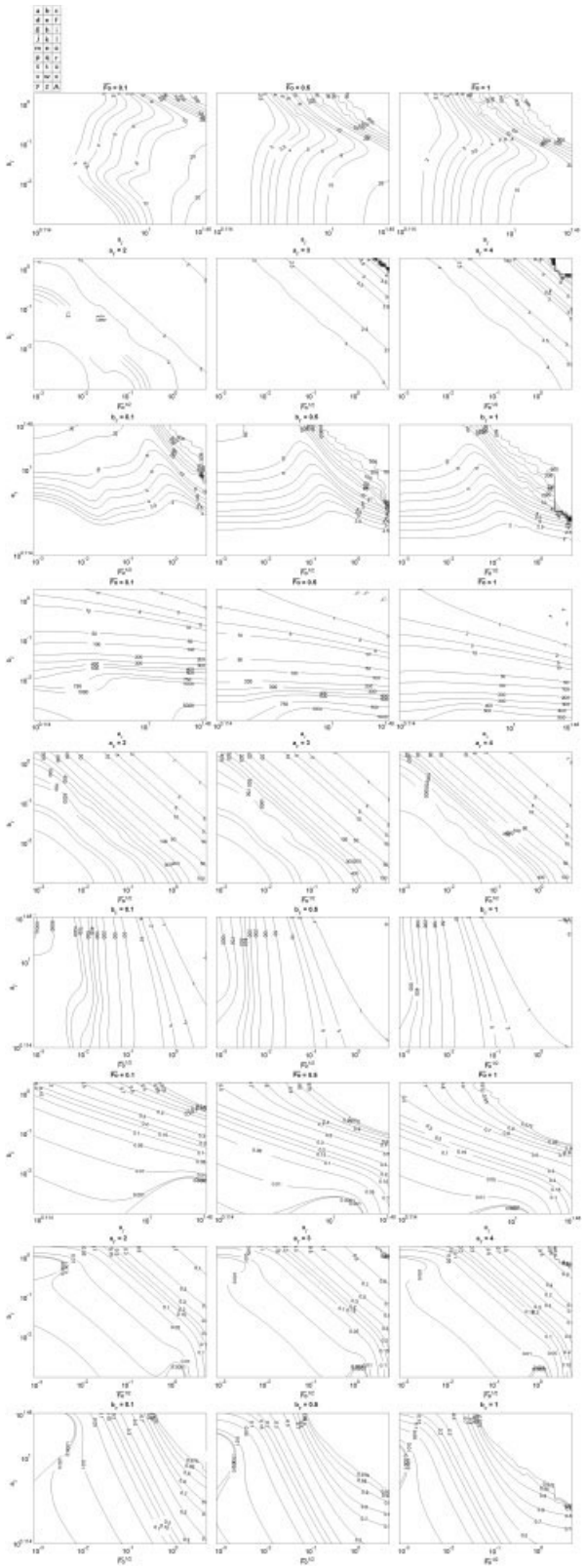

Figure 13. Fitted parameters a_β, b_β, and corresponding 50th percentile values x_{50} that approximate the pdf of $\bar{v}^*(\overline{Fo}, a_\Gamma, b_\Gamma)$ by $Beta(a_\beta, b_\beta)$ for the boundary condition BC_3.

(a–i) a_β isovalues, (j–r) b_β isovalues, (s–A) x_{50} values.

Conclusions

This work aims to contribute to the development of a generic approach for the quantitative assessment of the sanitary risk associated with the migration into foodstuffs of substances from food contact materials. The risk is evaluated in terms of cumulative quantity of migrant in food (that is, contamination level), starting from a stochastic resolution of transport and mass balance equations. In contrast with conventional migration models that predict point estimates of the contamination at given times for a given initial state, the proposed quantitative methodology relates the probability distributions of physical quantities (initial condition, boundary conditions, transport properties) to the probability distribution of the contamination. To reduce the number of inputs and to provide reliable calculation procedures, the proposed methodology is based on a dimensionless physical formulation where the variabilities and/or uncertainties in each quantity are formulated as a multiplicative contribution.

All quantities involved in the physical formulation are assumed to be distributed with respect to continuous laws and defined by experts. The results showed that the distribution of dimensionless $Fo^{1/2}$ number was reliably approximated by a Gamma distribution as an upper limit of the "true" distribution. An attractive characteristic of such a distribution is that the sum of k square roots of Fo numbers (such as that corresponding to k^2 days of storage) with a same Gamma(α, β) distribution (such as that corresponding to 1 day of storage) is Gamma($k\cdot\alpha$, β) distributed. From mass balance considerations, it is demonstrated that the dimensionless migration level, $\bar{v}^*$, is Beta distributed and therefore controlled by two scalar quantities, whatever the chosen transport equation and boundary conditions. Such a strong result is used to provide general abacuses that make it possible to calculate in a three-step procedure either the migration risk or the migration level for three realistic boundary conditions. The first step consists in calculating the scale parameter $\overline{Fo}^{1/2} = (\bar{D}\cdot\bar{t})^{1/2}/\bar{l}$ from the typical D, t, and l values. The second stage implies the inference of the parameters (a_Γ, b_Γ) of the distribution of $(Fo/\overline{Fo})^{1/2}$, from Figure 9, with respect to the variability or uncertainty on quantities D, t, and l. In a third step, either the Beta parameters of the distribution of $\bar{v}^*$ or the migration level for a risk of 50% are estimated from the projected contour plots given in Figures 11, 12, and 13.

The concentration in food (c_F) is finally determined from the distribution of the product $c_0\cdot\bar{v}_\infty\cdot\bar{v}^*$. If $c_0\cdot\bar{v}_\infty$ cannot be assumed to be δ distributed, the corresponding distribution of c_F may be calculated either from Eq. 7 or recursively from the approach detailed in the third section. In other cases, the distributions $c_F/(c_0\cdot\bar{v}_\infty)$ and $\bar{v}^*$ are identical.

The full approach for the estimation of c_F is illustrated for three arbitrary but realistic classes of food contact based on considerations about variability/uncertainty on kinetic input parameters. Two particular conditions are detailed, depending on the meaning of the distribution related to the parameter $D/\bar{D}$. Because the results (Figures 4–7) are presented in a dimensionless form, with respect to the value of $\overline{Fo}$, they may used to perform (1) a sanitary survey of packed foods and (2) a selection of providers or materials. This preliminary theoretical work is currently applied to estimate the possible contamination of each packed food consumed by a French panel of about 6000 households during one year. Twelve typical packed foods and two typical migrants were defined and the contamination is calculated from Eq. 6, with respect to the contact time between the food and the packaging material, and by taking into account the uncertainty on c_0 and D values. Conclusions will be used to appraise consumer exposure to food packaging substances (to be published).

Literature Cited

1. Harison H. Migration of plasticizers from cling-film. *Food Addit Contam.* 1988;5:493-499.
2. Petersen JH, Breindahl T. Plasticizers in total diet samples, baby food and infant formulae. *Food Addit Contam.* 2000;17:133-141.
3. Sharman M, Readn WA, Castle L, Gilbert J. Levels of di-(2-ethylhexyl)phthalate and total phthalate esters in milk, cream, butter and cheese. *Food Addit Contam.* 1994;11:375-385.
4. Castle L, Mayo A, Gilbert J. Migration of plasticizers from printing inks into foods. *Food Addit Contam.* 1989;6:437-443.
5. European Commission, Health & Consumer Protection Directorate-General (EC-DG SANCO-D3). Conclusions of the workshop CANCO: Can coatings for direct food contact. EU-QLAM-2001-00066, Brussels, Belgium: EC; 2002.
6. Fantoni L, Simoneau C. Contamination of baby food by epoxydised soybean oil. Proc of 6th International Symposium of Food Authenticity and Safety, Nantes, France, Nov. 28–30; 2001.
7. Simoneau C, Theobald A, Wiltschko D, Anklam E. Estimation of intake of BADGE from canned fish consumption in Europe and migration survey. *Food Addit Contam.* 1999;16:457-463.
8. International Agency for Research on Cancer (IARC). *IARC Monographs on the Evolution of Carcinogenic Risks to Humans to Some Industrial Chemicals*, Vol. 77. Lyon, France: IARC Press; 2000.
9. Colerangle JB, Roy D. Profound effects of the weak environmental estrogen-like chemical bisphenol A on the growth of the mammary gland of noble rats. *J Steroid Biochem Mol Biol.* 1997;60:153-160.
10. EU Commission Directive 89/109/EEC of Feb. 11, 1989 relating to the approximation of the laws of the Member States relating to materials and articles intended to come into contact with foodstuffs, O.J. L40; 1989:38.
11. EC-DG SANCO-D3. Conclusions of the thematic network: Evaluation of migration models to be used under Directive 90/128/EEC, SMT-CT98-7513. Brussels, Belgium: EC; 2002.
12. Karayiannis NC, Mavrantzas VG, Theodorou DN. Diffusion of small molecules in disordered media: Study of the effect of kinetic and spatial heterogeneities. *Chem Eng Sci.* 2001;56:2789-2801.
13. Yeo GF, Milne RK. On characterizations of beta and gamma distributions. *Stat Probabil Lett.* 1991;11:239-242.

Manuscript received Sept. 2, 2003, revision received July 27, 2004, and final revision received Dec. 3, 2004.